Inorganic Chemistry

pubs.acs.org/IC
Article

Hydrogen Activation with Ru-PN^{3}P Pincer Complexes for the Conversion of C_1 Feedstocks

Matthew D. Morton, Boon Ying Tay, Justin J.Q. Mah, Andrew J.P. White, James D. Nobbs,* Martin van Meurs, and George J.P. Britovsek*

Cite This: *Inorg. Chem.* 2024, 63, 3393−3401

ABSTRACT: The hydrogenation of C_1 feedstocks (CO and CO_2) has been investigated using ruthenium complexes [RuHCl(CO)(PN^{3}P)] as the catalyst. PN^{3}P pincer ligands containing amines in the linker between the central pyridine donor and the phosphorus donors with bulky substituents (*tert*-butyl (**1**) or TMPhos (**2**)) are required to obtain mononuclear single-site catalysts that can be activated by the addition of KO^{t}Bu to generate stable five-coordinate complexes [RuH(CO)(PN^{3}P−H)], whereby the pincer ligand has been deprotonated. Activation of hydrogen takes place via heterolytic cleavage to generate [RuH$_2$(CO)(PN^{3}P)], but in the presence of CO, coordination of CO occurs preferentially to give [RuH(CO)$_2$(PN^{3}P−H)]. This complex can be protonated to give the cationic complex [RuH(CO)$_2$(PN^{3}P)]$^+$, but it is unable to activate H_2 heterolytically. In the case of the less coordinating CO_2, both ruthenium complexes **1** and **2** are highly efficient as CO_2 hydrogenation catalysts in the presence of a base (DBU), which in the case of the TMPhos ligand results in a TON of 30,000 for the formation of formate.

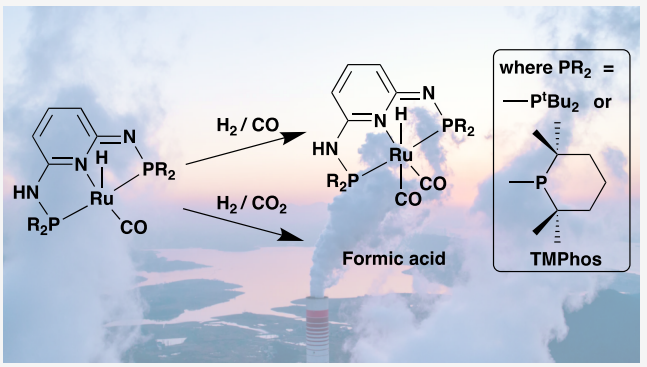

INTRODUCTION

The efficient production of green hydrogen and its conversion to renewable liquid energy carriers such as formic acid or methanol, so-called power-to-liquids (P2L) processes, are gaining increased interest due to the urgent need for sustainable fuels.[1−3] Green hydrogen refers to H_2 obtained from a renewable source, for example, through water electrolysis using renewable electricity or from the gasification of biomass. Hydrogenations of C_1 feedstocks such as CO or CO_2 are important in this context as this can give access to a range of green chemicals, including HCO_2H, MeOH, and hydrocarbons.[4−8] The hydrogenation of CO is currently applied in several large-scale chemical processes such as the Fischer−Tropsch process and the production of MeOH (110 Mt per annum),[9] all based on heterogeneous catalysis. Likewise, the industrial hydrogenation of CO_2 to CH_4[10] or MeOH[11] also utilizes heterogeneous catalysis. Although at a much smaller scale of deployment as compared to that of CO, CO_2 is becoming an increasingly important feedstock. The synthesis of MeOH appears to be the most attractive, exemplified by the 5,000 tons per annum plant operated by CRI in Iceland and other demonstration plants.[11,12] With advances in the efficiencies of electrolyzers and hydrogenation technologies, CO_2 hydrogenation to green methanol or dimethyl ether (DME) is likely to become increasingly important in the near future. Longer term, this could result in a MeOH-based economy as originally envisaged by Asinger in 1986,[13] and later also by Olah et al.[14]

Efficient homogeneous systems capable of hydrogenation reactions of these C_1 feedstocks have long remained elusive, despite the heterogeneous systems being well established, in some cases for more than a century. However, recently there have been some exciting discoveries of molecular catalysts that can reduce CO to MeOH via formamide or formate intermediates.[15−17] These discoveries have occurred in tandem with significant advances in homogeneous hydrogenation of CO_2 to MeOH in the past decade.[18]

The catalytic hydrogenation of CO and CO_2 feedstocks both require heterolytic cleavage of H_2 to generate hydride and proton donors. Pincer ligands of the types **PCNCP** and **PN^{3}P** such as those shown in Scheme 1 and similar PNN systems,[19] as well as the related **MACHO** ligand types,[20−24] have featured prominently in this area as they can be reversibly protonated and deprotonated.[25−30] This has made these ligands particularly attractive for hydrogenations using H_2 activation

Received: November 13, 2023
Revised: January 18, 2024
Accepted: January 23, 2024
Published: February 8, 2024

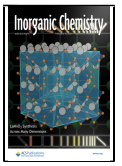

Scheme 1. Reversible Deprotonation and H_2 Activation through Metal Ligand Cooperativity in MACHO, PCNCP, and PN^3P Pincer Complexes

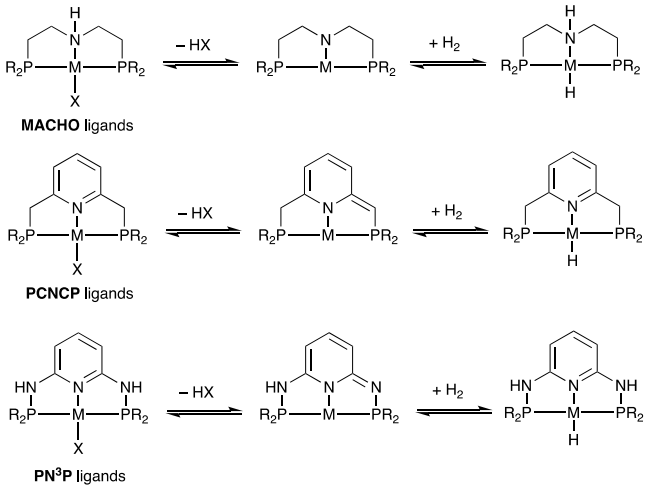

reactions via metal–ligand cooperative (MLC) behavior,[31−34] although recent discoveries suggests that this MLC behavior may not be essential for all catalyst systems.[23] Here, we present our studies on the synthesis of a series of ruthenium(II) complexes featuring PN^3P-R ligands (where R = ^{t}Bu and TMPhos[35]) and their reactivity toward H_2 and CO, as well as their application in the hydrogenation of CO and CO_2.

RESULTS AND DISCUSSION

Synthesis and reactivity of PN^3P Ru complexes. [RuHCl(CO)(PN^3P-^{t}Bu)] (**1**) was prepared by mixing a PN^3P-^{t}Bu ligand with [RuHCl(CO)(PPh_3)$_3$] in THF according to the procedure described by Huang et al. and shown in Scheme 2.[36] The ^{1}H NMR spectrum (d_4-MeOH) shows a distinctive hydride signal at −24.1 ppm (triplet, $^2J_{HP}$ = 18 Hz) and a doublet in the ^{31}P NMR spectrum at 134 ppm ($^2J_{PH}$ = 18 Hz). In d_6-benzene or $CDCl_3$ instead of d_4-MeOH, the NH protons are observed as a broad singlet. The IR spectrum shows a CO stretch at 1936 cm^{-1}, and the Ru–H stretch is seen at 2113 cm^{-1}. All data is shown in the Supporting Information and is consistent with that reported by Huang and co-workers.[36]

Scheme 2. Synthesis of Ru-PN^3P Complexes 1 and 2

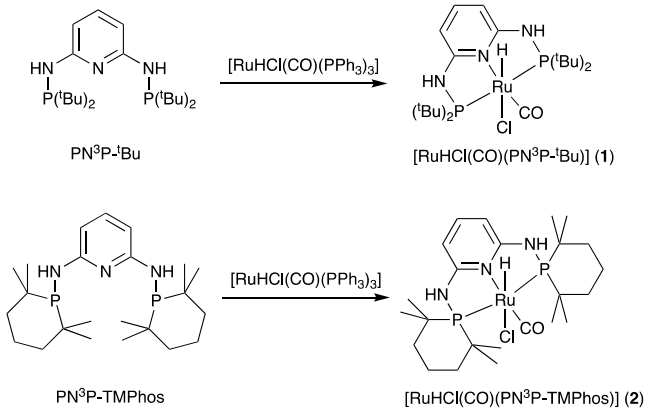

An alternative bulky phosphine 2,2,6,6-tetramethylphosphinane (TMPhos), recently developed by some of us,[35] was also investigated as it provides a similar but subtly different stereoelectronic environment compared to P^{t}Bu$_2$ groups. The new ligand PN^3P-TMPhos was obtained in 47% yield from 2,6-diaminopyridine and chloro-TMPhos (1-chloro-2,2,6,6-tetramethylphosphinane). The reaction with PN^3P-TMPhos proceeds in a similar fashion as above resulting in [RuHCl(CO)(PN^3P-TMPhos)] (**2**) (Scheme 2). Interestingly, the hydride signal appears much further downfield in this case at −14.4 ppm ($^2J_{HP}$ = 20 Hz, d_3-MeCN), together with a significantly lower Ru–H stretching frequency at 2070 cm^{-1}. The ^{31}P NMR signal at 124 ppm and the carbonyl stretch at 1932 cm^{-1} are comparable to those of [RuHCl(CO)(PN^3P-^{t}Bu)] (**1**).

Similar reactions using the related PN^3P-^{i}Pr and -Ph ligands were also attempted but were largely unsuccessful. The reaction of PN^3P-^{i}Pr with [RuHCl(CO)(PPh_3)$_3$] in refluxing THF led to a mixture of the desired complex [RuHCl(CO)(PN^3P-^{i}Pr)] and presumably the cationic complex [RuH(CO)(PPh_3)(PN^3P-^{i}Pr)]Cl, as well as other unidentified byproducts (see Figures S23 and S24). The reaction between PN^3P-Ph and [RuHCl(CO)(PPh_3)$_3$] gave the cationic complex [RuH(CO)(PPh_3)(PN^3P-Ph)]Cl with some unidentified species (Figures S26 and S27). Similar issues in the synthesis of Ru complexes with the PN^3P-Ph ligand have been reported, and a dinuclear Ru complex with a bridging PN^3P ligand was isolated.[26] Kirchner and co-workers synthesized the [(PN^3P)RuCl$_2$] complexes from [RuCl$_2$(PPh_3)$_3$], which avoided the CO ligand.[37]

Treatment of [RuHCl(CO)(PN^3P-^{t}Bu)] (**1**) with KO^{t}Bu results in the formation of the five-coordinate complex [RuH(CO)(PN^3P-^{t}Bu–H)] (**3**) (Scheme 3). The ^{1}H NMR spectrum of [RuH(CO)(PN^3P-^{t}Bu–H)] in d_6-benzene shows a loss of symmetry in the aromatic region, and the hydride signal is shifted upfield to −25.9 ppm ($^2J_{HP}$ = 16 Hz) (Figure S5). The ^{31}P{^{1}H} NMR spectrum shows two doublets at 128.2 and 130.7 ppm ($^2J_{PP}$ = 220 Hz). The IR spectrum shows a single CO stretch at 1885 cm^{-1}, which is 50 cm^{-1} lower than that for [RuHCl(CO)(PN^3P-^{t}Bu)] (**1**), suggesting greater back-bonding to CO. Similarly, [RuH(CO)(PN^3P-TMPhos–H)] (**4**) can be generated from [RuHCl(CO)(PN^3P-TMPhos)] (**2**) and 1 equiv of KO^{t}Bu. The protons in the dearomatized pyridine ring see an upfield shift from 7.16 and 6.72 ppm to 6.83 and 5.77 ppm, respectively, while the hydride signal shifts slightly upfield from −14.4 to −14.5 ppm ($^2J_{HP}$ = 19 Hz). The ^{31}P{^{1}H} NMR spectrum shows a broad singlet at 122.1 ppm in contrast to the two doublets observed for the ^{t}Bu complex **3**, which suggests fluxional behavior in CD_3CN, similar to that observed for the CO-coordinated complex **5** (*vide infra*). We found that complex **4** is thermally unstable and gradually decomposes in solution.

The reaction of [RuH(CO)(PN^3P-^{t}Bu–H)] (**3**) with CO (1 bar) at room temperature (RT) in C_6D_6 resulted immediately in a color change from red to pink/orange and the formation of a dicarbonyl complex [RuH(CO)$_2$(PN^3P-^{t}Bu–H)] (**5**) (Scheme 3). Complex **5** is also obtained from the reaction between PN^3P-^{t}Bu and [Ru$_3$(CO)$_{12}$] in toluene at 110 °C. In contrast, the reaction of PN^3P-^{i}Pr with [Ru$_3$(CO)$_{12}$] in refluxing toluene resulted in complicated mixtures of products (see Figure S25). The ^{1}H NMR spectrum in C_6D_6 of [RuH(CO)$_2$(PN^3P-^{t}Bu–H)] (**5**) is similar to the spectrum of [RuH(CO)(PN^3P-^{t}Bu–H)] (**3**) (see Figure S32), but the signals for the aromatic protons in 3 and 5 position and the *tert*-butyl groups are all broader. The hydride appears as a

https://doi.org/10.1021/acs.inorgchem.3c04001
Inorg. Chem. 2024, 63, 3393−3401

Scheme 3. Reaction of Complexes 1 and 2 with KO^{t}Bu and Subsequent Reactivity

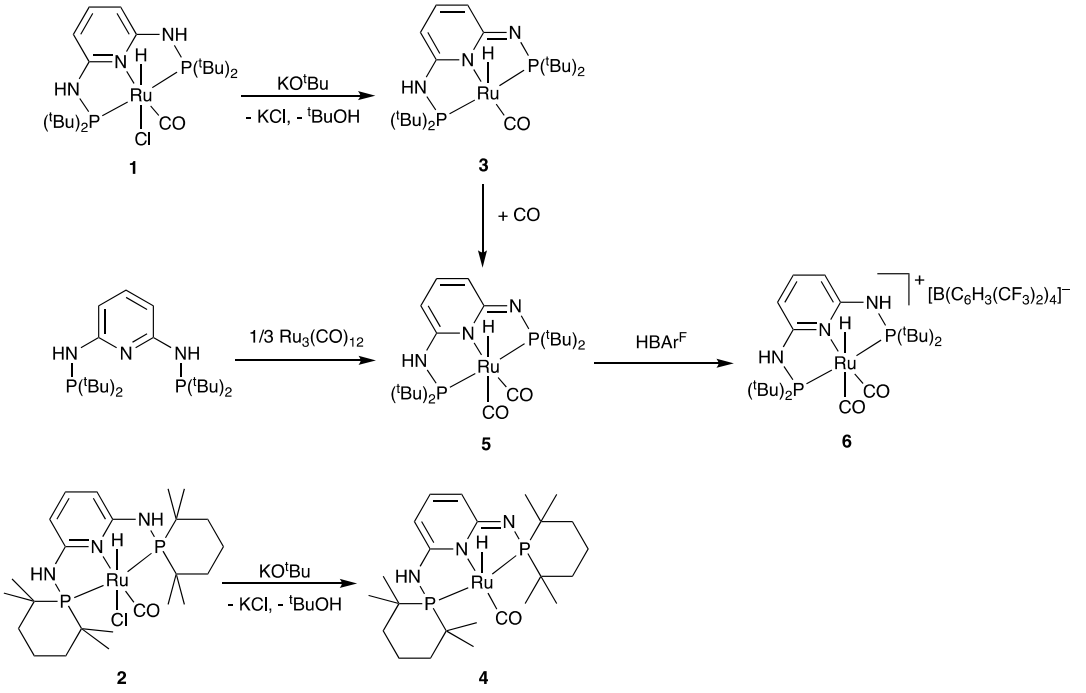

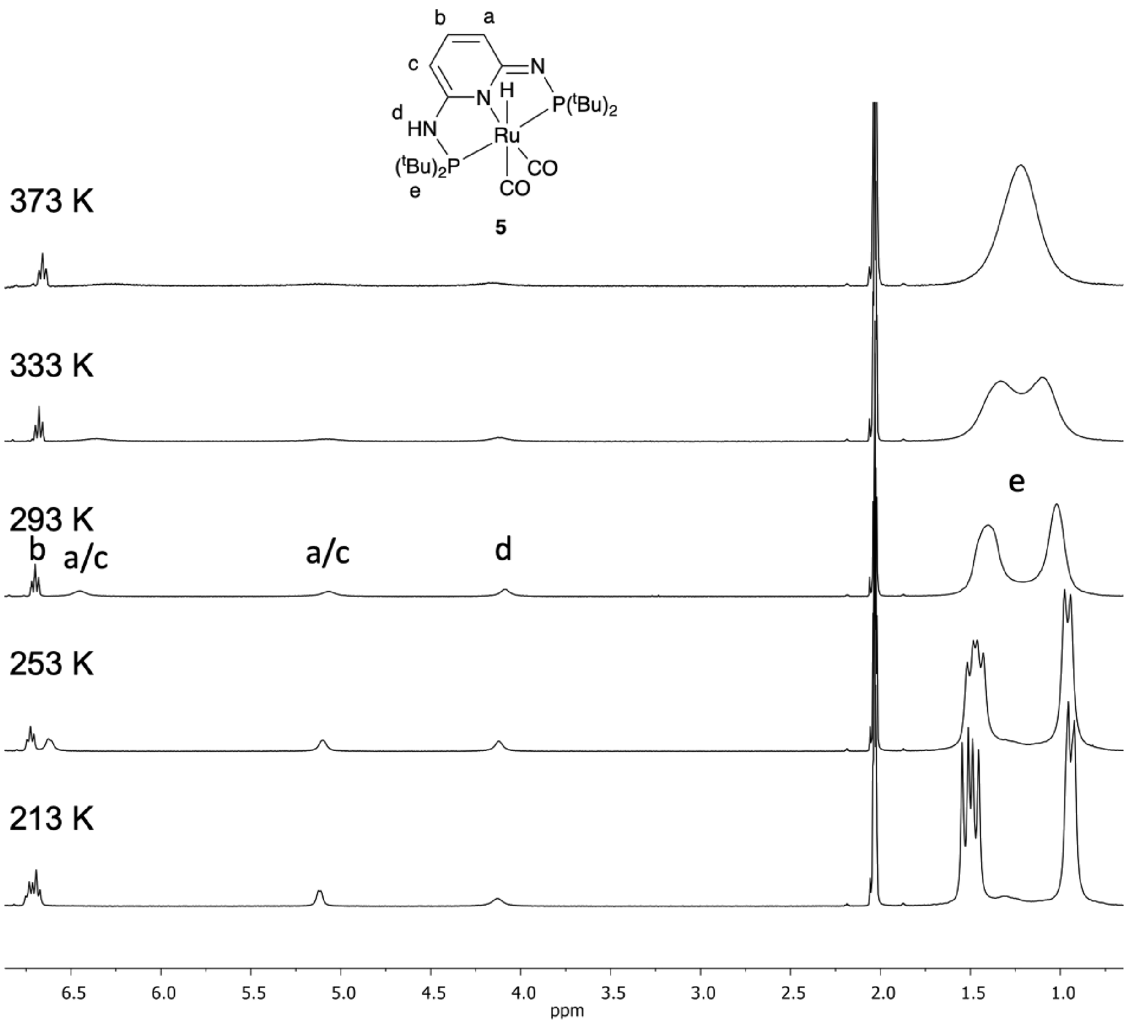

Figure 1. Variable temperature ^{1}H NMR spectra of [RuH(CO)$_2$(PN^{3}P-^{t}Bu−H)] (**5**) in d_8-toluene (hydride signal has been omitted).

https://doi.org/10.1021/acs.inorgchem.3c04001
Inorg. Chem. 2024, 63, 3393−3401

triplet at −6.1 ppm ($^2J_{HP}$ = 19 Hz), significantly downfield from −25.9 ppm in starting monocarbonyl complex **3**, probably due to the *trans* effect of the second carbonyl ligand. The $^{31}P\{^1H\}$ NMR spectrum (C_6D_6) shows two doublets at 135.2 and 140.9 ppm ($^2J_{PP}$ = 190 Hz), which are also broadened. There are two $\nu_{(CO)}$ absorptions at 1989 and 1940 cm^{-1} in the IR spectrum.

The dicarbonyl complex [RuH(CO)$_2$(PN^{3}P-^{t}Bu-H)] (**5**) shows fluxional behavior in solution at RT, which was investigated by variable temperature ^1H NMR spectroscopy in d_8-toluene (see Figure 1). At 213 K, the broad peaks are better resolved although not completely sharp. Increasing the temperature results in further broadening and coalescence of the *tert*-butyl groups at 373 K. The ^{31}P NMR spectra show two sharp doublets at low temperatures and two broad doublets at higher temperatures, but no coalescence is observed up to 373 K.

At all measured temperatures, the ^1H NMR spectra show the pyridine proton in the 4 position as a triplet at 6.7 ppm and the hydride as a triplet at −6 ppm, and both are sharp signals. The fluxionality is proposed to involve proton transfer between the imine and amine moieties of the ligand, interconverting between the two enantiomeric forms of the complex, as shown in Scheme 4. Noteworthy, there was no fluxional behavior reported for the related complex [RuH(CO)(PPh$_3$)(PN^{3}P-Ph−H)].[26]

Scheme 4. Equilibrium between the Two [RuH(CO)$_2$(PN^{3}P-^{t}Bu−H)] (5) Isomers (Protons in Blue Show Exchange Behavior)

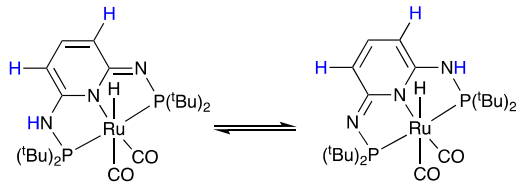

No evidence for an intermediate was observed, for example, a Ru(0) complex [Ru(CO)$_2$(PN^{3}P-^{t}Bu)], which would be structurally similar to the [Ru(CO)$_2$(PONOP-^{t}Bu)] complex reported by Milstein et al.[38] The ^1H and ^{31}P NMR spectra of [RuH(CO)$_2$(PN^{3}P-^{t}Bu−H)] (**5**) were also measured in d_4-methanol, where complete coalescence for the ^{t}Bu signals is observed at RT. This indicates that the fluxional process most likely involves proton exchange with methanol facilitating the proton transfer from one side of the ligand to the other. The free energy of activation ($\Delta G^{\ddagger}$) for the exchange process in d_8-toluene was determined by NMR as 73 kJmol^{-1} (see the Supporting Information for details).

Protonation of [RuH(CO)$_2$(PN^{3}P-^{t}Bu−H)] (**5**) with a strong acid [H(OEt$_2$)$_2$][B(C$_6$H$_3$(CF$_3$)$_2$)$_4$] (HBAr^F) in THF results in the cationic complex [RuH(CO)$_2$(PN^{3}P-^{t}Bu)]$^+$ (**6**) in good yield (78%). The ^1H NMR spectrum (C_6D_5Cl) is consistent with the rearomatization of the complex, resulting in a symmetric complex with only one signal for the protons in 3 and 5 position and a singlet in the $^{31}P\{^1H\}$ NMR spectrum at 142.7 ppm. No fluxional behavior was seen for this complex. The CO stretches in the IR spectrum are at 2017 and 1986 cm^{-1}, which are 40 cm^{-1} higher than for the neutral complex [RuH(CO)$_2$(PN^{3}P-^{t}Bu−H)] (**5**). The cationic complex **6** was further characterized by ^{13}C NMR spectroscopy, mass spectrometry, elemental analysis, and SC-XRD (see the Supporting Information and Figure 2). The octahedral complex shows different Ru−C bond lengths, whereby the

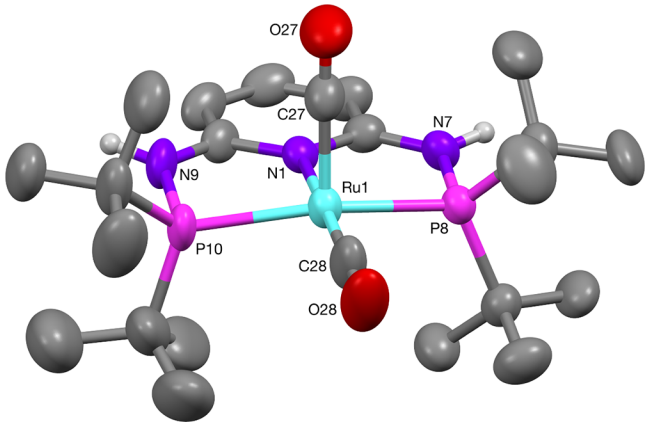

Figure 2. Molecular structure of the cationic complex [RuH(CO)$_2$(PN^{3}P-^{t}Bu)]$^+$ (**6**). The exact position of the hydride ligand could not be determined (Supporting Information). The anion [B(C$_6$H$_3$(CF$_3$)$_2$)$_4$]$^-$ has been omitted for clarity. Selected bond lengths (Å) and angles (deg): Ru(1)−C(28) 1.878(8), Ru(1)−C(27) 1.976(8), Ru(1)−N(1) 2.115(4), Ru(1)−P(8) 2.345(3), Ru(1)−P(10) 2.357(3); C(28)−Ru(1)−C(27) 95.6(4), P(8)−Ru(1)−P(10) 156.02(15), and C(28)−Ru(1)−N(1) 175.1(4).

axial Ru−C bond *trans* to the hydride ligand is significantly longer at 1.976(8) Å, compared to the equatorial Ru−C bond at 1.878(8) Å. Related cationic complexes [RuH(CO)$_2$(PNP-R)]$^+$ with a different PNP-pincer-type ligand that features a central NH donor have been reported.[20,39] In all cases, the Ru−C bond length of the axial CO ligand is significantly longer than that of the equatorial CO ligand by approximately 0.1 Å due to the *trans* hydride ligand.

Hydrogen and CO Activation. The hydrogenation of CO with homogeneous transition metal-based catalysts to generate MeOH and further homologation products such as ethylene glycol is generally believed to proceed via the reaction sequence shown in Scheme 5. Formyl and hydroxymethyl complexes are generally invoked as intermediates in these reactions.[40−42] Transition metal hydrides have been used by Bercaw et al. in homogeneous syngas conversion in combination with metal carbonyl complexes based on group 7 metals Re[43] and Mn.[44]

The reactivity of [RuH(CO)(PN^{3}P-^{t}Bu−H)] (**3**) toward H$_2$ was explored in a series of stoichiometric reactions. The reaction between **3** and H$_2$ (5 bar) was monitored by ^1H and ^{31}P NMR spectroscopy in C_6D_6. Immediately after the addition of H$_2$, a new triplet is observed in the ^1H NMR spectrum at −5.3 ppm ($^2J_{HP}$ = 19 Hz) and a new set of aromatic signals appears as a triplet and a doublet in a 1:2 ratio. A singlet is observed in the $^{31}P\{^1H\}$ NMR spectrum at 156.2 ppm. However, this reaction is slow, as noted by Huang et al.,[45] and only approximately 1% conversion was observed after 1 h, but after 4 days at RT under H$_2$, this increased to 10% (see Figures S19 and S20). Based on these observations, we assign the new signals to the symmetric *trans*-dihydride complex [Ru(H)$_2$(CO)(PN^{3}P-^{t}Bu)] (**7**). Heating to 60 °C for 30 min resulted in decomposition of [RuH(CO)(PN^{3}P-^{t}Bu−H)] (**3**) rather than further reaction with H$_2$ to generate more **7**. Repeating the experiment above with D$_2$ instead of H$_2$ resulted in a gradual decrease in the intensity of the hydride and the

https://doi.org/10.1021/acs.inorgchem.3c04001
Inorg. Chem. 2024, 63, 3393−3401

Scheme 5. Proposed Reaction Sequence for the Hydrogenation of CO to MeOH and Higher Alcohols

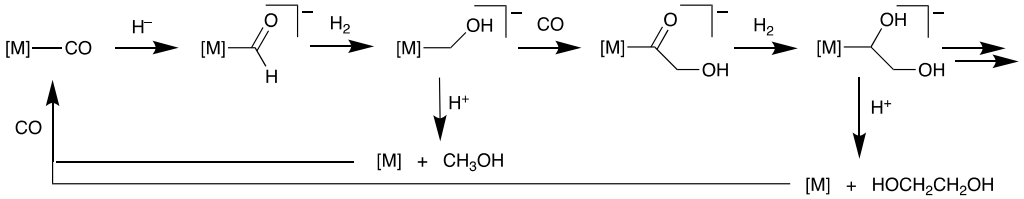

NH signals relative to the aromatic proton signals. This indicates that the H_2 activation is reversible and there is an equilibrium between the two complexes in solution under H_2, as indicated in Scheme 6. A direct synthesis of complex

Scheme 6. Reactivity of Complex 3 toward H_2 in the Absence and Presence of CO

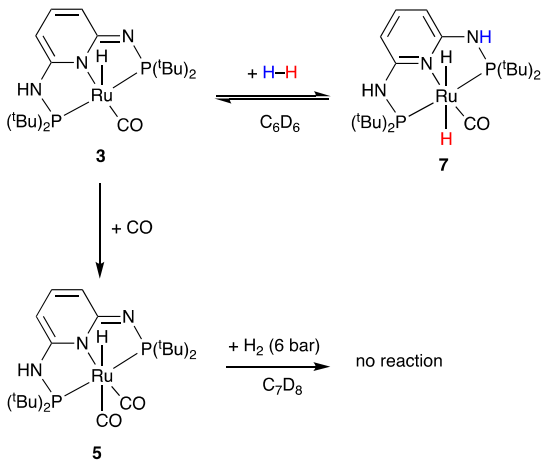

$[Ru(H)_2(CO)(PN^3P\text{-}^tBu)]$ (**7**) was attempted by reacting complex $[RuHCl(CO)(PN^3P\text{-}^tBu)]$ (**1**) with $NaBEt_3H$ in toluene, as reported for the related $[Ru(H)_2(CO)(PONOP\text{-}^tBu)]$ complex,[38] but the major product observed in this case was the five-coordinate complex $[RuH(CO)(PN^3P\text{-}^tBu{-}H)]$ (**3**). It is possible that complex **7** was formed as an intermediate but reverts immediately back to complex **3** in the absence of excess H_2. The reaction of the dicarbonyl complex $[RuH(CO)_2(PN^3P\text{-}^tBu{-}H)]$ (**5**) with H_2 (6 bar, in d_8-toluene) was unsuccessful, and no reaction was observed during 48 h at RT or after 30 min at 60 °C.

We subsequently explored the possibility of using a dual catalyst system, where one complex activates H_2 and the other activates CO. The first system combines the ability of $[RuH(CO)(PN^3P\text{-}^tBu{-}H)]$ (**3**) to activate H_2 and subsequently engage in intermolecular hydride transfer to other carbonyl complexes. Initially, we chose the Ru-bipy complex $[Ru(bipy)_2(CO)_2](B(C_6F_5)_4)_2$ (**8**) as a previous work by Tanaka and co-workers has shown that the formation of the formyl complex $[Ru(bipy)_2(CO)(CHO)]^+$ can be achieved by stoichiometric borohydride reduction.[46] In an attempt to obtain a similar reduction using H_2 instead of $NaBH_4$, we reacted $[Ru(bipy)_2(CO)_2](B(C_6F_5)_4)_2$ (**8**) with $[RuH(CO)(PN^3P\text{-}^tBu{-}H)]$ (**3**) in the presence of H_2 (4 bar) in C_6D_5Cl at RT according to Scheme 7.

The reaction of $[Ru(bipy)_2(CO)_2](B(C_6F_5)_4)_2$ (**8**) and $[RuH(CO)(PN^3P\text{-}^tBu{-}H)]$ (**3**) with H_2 leads to an instant conversion to the formyl complex $[Ru(bipy)_2(CO)(CHO)]^+$ (**9**) as indicated by the characteristic singlet at 13.9 ppm[47] together with the cationic Ru complex **10** (see Figure S33). This signal disappears over the course of several hours due to decarbonylation to form $[Ru(bipy)_2(CO)(H)]^+$ (**11**) evidenced by the emergence of the Ru-hydride signal at −11.4 ppm[48] and $[RuH(CO)_2(PN^3P\text{-}^tBu)]^+$ (**6**) at −6.7 ppm. The thermal instability of the formyl complex $[Ru(bipy)_2(CO)(CHO)]^+$ (**9**) has been noted previously.[47] Another experiment was performed by reacting $[Ru(bipy)_2(CO)_2](B(C_6F_5)_4)_2$ (**8**) and $[RuH(CO)(PN^3P\text{-}^tBu{-}H)]$ (**3**) with syngas (CO/H_2 = 3/1), which formed $[RuH(CO)_2(PN^3P\text{-}^tBu{-}H)]$ (**5**) instantaneously, precluding any further heterolytic cleavage of H_2.

Inspired by Dombek's early observations on the formation of MeOH and ethylene glycol from $[Ru_3(CO)_{12}]$ and syngas,[49]

Scheme 7. Hydride Transfer to Generate Metal Formyl Intermediates and Subsequent Decarbonylation

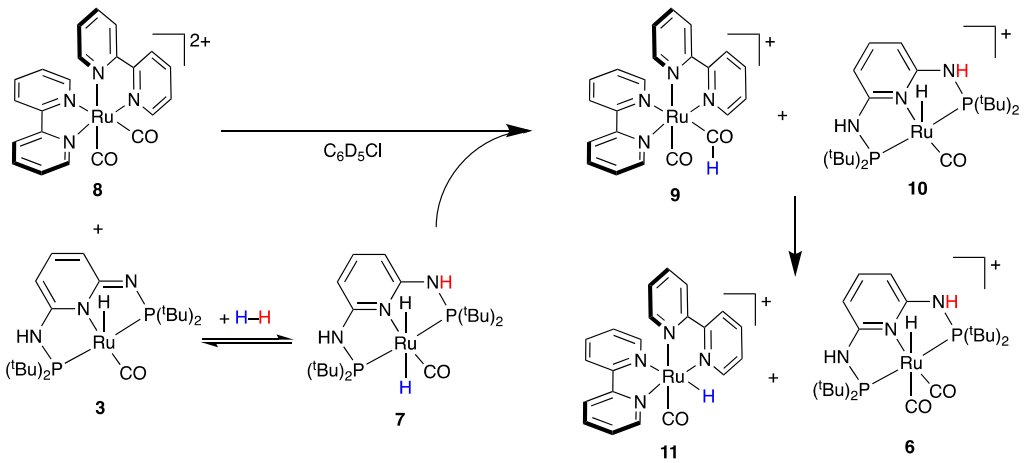

https://doi.org/10.1021/acs.inorgchem.3c04001
Inorg. Chem. 2024, 63, 3393−3401

Scheme 8. Hydride Transfer to $[Ru_3(CO)_{12}]$

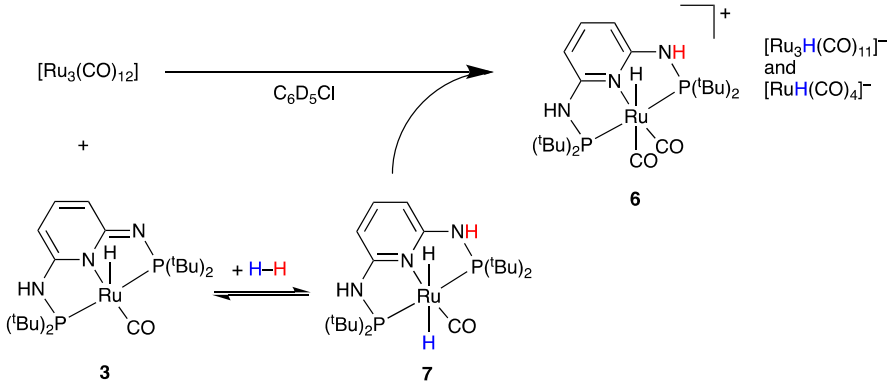

albeit under forcing conditions, we attempted the hydrogenation of $[Ru_3(CO)_{12}]$ in the presence of [RuH(CO)-(PN^3P-^{t}Bu–H)] (**3**) at RT (Scheme 8). Upon introduction of H_2 (1 bar), fast H_2 activation to give $[RuH_2(CO)(PN^3P$-^{t}Bu)] (**7**) was followed by a slow hydride and CO exchange with $[Ru_3(CO)_{12}]$ to generate the known anionic complexes $[Ru_3H(CO)_{11}]^-$ and $[RuH(CO)_4]^-$.[50,51] It is possible that this exchange also involves metal formyl species as intermediates. Before H_2 addition, some CO exchange was observed to form small amounts of $[RuH(CO)_2(PN^3P$-^{t}Bu–H)] (**5**) (see Figure S34).

From these stoichiometric reactivity studies, it can be concluded that pincer complexes such as [RuH(CO)-(PN^3P-^{t}Bu–H)] (**3**) are able to activate H_2 to give $[Ru(H)_2(CO)(PN^3P$-^{t}Bu)] (**7**), but no hydride transfer to the coordinated carbonyl ligand is observed. The activated complex **7** is able to transfer hydride equivalents to other metal carbonyl complexes to generate metal formyl intermediates, but these tend to be unstable at higher temperatures. More importantly, when using syngas, H_2 activation becomes inhibited due to the preferential coordination of CO. Higher partial pressures of H_2 may be needed to overcome this and displace coordinated CO. The hydrogenation of CO_2 however should proceed as long as no CO is present as one of the reaction products.

Hydrogenation of CO_2 to Formate. Huang and co-workers have shown previously that Ru complex **1** is an efficient catalyst for H_2 generation from the decomposition of HCO_2H (TON > 1 million).[45] Since equimolar CO_2 is also generated, the reverse reaction, i.e., hydrogenation of CO_2, would be needed for HCO_2H to be feasible as a renewable H_2/energy carrier. However, direct conversion of CO_2 to formic acid is endergonic and therefore a base or high pressures are usually employed to drive the forward reaction.[6,7,52] Pidko and co-workers have demonstrated that related Ru-PNP-pincer catalysts are highly efficient in the base-assisted hydrogenation of CO_2 to formates with reported mol DBU-formate/(mol cat x h) (TOFs) in excess of 1 million h^{-1} at exceptionally low Ru loadings (<0.2 μmol).[25]

We have investigated complexes **1** and **2** as catalysts for the CO_2 hydrogenation reaction, and the results are shown in Table 1. In a typical experiment, the precatalyst, dissolved in the reaction solvent dimethylformamide (DMF), was introduced into a batch reactor together with the base 1,8-diazabicyclo[5.4.0]undec-7-ene (DBU). After heating to the reaction temperature (90 °C), a mixture of CO_2/H_2 (7.5/7.5 bar) was introduced into the reactor and maintained at this

Table 1. Base-Assisted Hydrogenation of CO_2 to Formate Using Complexes 1 and 2[b]

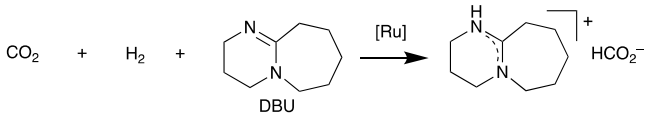

entry	catalyst	[Ru] μmol	conversion[a] (%)	TON[b]
1	blank	0	0	0
2	**1**	14.2	93	4400
3	**2**	14.2	>99	4700
4	**1**	5.7	>99	11,800
5	**2**	5.7	>99	11,800
6	**1**	2.8	10	2300
7	**2**	2.8	100	23,600
8	**1**	1.4	0.3	100
9	**2**	1.4	64	30,300

[a]conversion = DBU-formate/DBU × 100. [b]TON = mol DBU-formate/mol cat. [c]Conditions: CO_2/H_2 (1:1) = 15 bar, temp. = 90 °C, reaction time = 1 h, DBU = 10 mL (66.9 mmol), solvent = DMF (35 mL).

pressure throughout the reaction. In the absence of any catalyst (entry 1), negligible gas consumption was observed, although a small amount of white solid was formed, likely to be DBU-bicarbonate $[(DBU)H]^+[HCO_3]^-$ resulting from trace amounts of moisture in the system.[53] Gratifyingly, both catalysts **1** and **2** were highly efficient in the DBU-assisted hydrogenation of CO_2 to formate. Quantitative conversion of DBU was observed within 1 h at catalyst loadings of >5 μmol (entries 2–5). At a catalyst loading of 14.2 μmol, catalyst **1** and **2** gave TONs of 4400 and 4700, respectively, reflecting >93% conversion of DBU. Even when the catalyst loading was lowered to 5.7 μmol, full conversion of DBU was observed for both complexes **1** and **2** equating to TONs of 11,800 (entries 4 and 5).

Since the reaction is limited by the amount of DBU, we lowered the catalyst loading further in order to differentiate between the performances of the two catalysts. At a lower catalyst loading of 2.8 μmol, using complex **1**, conversion of DBU decreased to 10% (entry 6), whereas with complex **2**, quantitative conversion of base was still achieved, with a TON of 23,600 (entry 7). At an even lower catalyst loading of 1.4 μmol, complex **1** was essentially inactive (entry 8), whereas complex **2** achieved 64% conversion of DBU and a TON of 30,300. Thus, both catalysts are highly efficient in the hydrogenation of CO_2 to DBU-formate with TONs > 30,000

https://doi.org/10.1021/acs.inorgchem.3c04001
Inorg. Chem. 2024, 63, 3393–3401

h^{-1} for complex **2**. At lower catalyst loadings, both complexes appear to be susceptible to deactivation, but catalyst **2** appears to be more robust in that respect.

CONCLUSIONS

We have shown that mononuclear Ru complexes with PN^3P-R pincer-type ligands can be prepared cleanly, provided that sterically bulky R groups are used such as *tert*-butyl or TMPhos. Smaller R groups such as ^{i}Pr and Ph lead to multiple products. Both six-coordinate complexes [RuClH(CO)(PN^3P-R)] (**1** and **2**) react with KO^{t}Bu to form the five-coordinate complexes [RuH(CO)(PN^3P-R−H)] (**3** and **4**). In the case of R = ^{t}Bu, reactivity studies with CO have shown that a dicarbonyl complex [$RuH(CO)_2(PN^3P$-^{t}Bu−H)] (**5**) is formed, which shows temperature-dependent dynamic behavior in solution and which can be protonated to give the cationic complex [$RuH(CO)_2(PN^3P$-^{t}Bu)]$^+$ (**6**). Dihydrogen is reversibly activated by complex **3** to give the dihydride complex [$RuH_2(CO)(PN^3P$-^{t}Bu)] (**7**). Attempts to use this dihydride complex as a hydride donor with other ruthenium carbonyl complexes led to unstable formyl complexes, which readily decarbonylated to give the stable cationic complex **6**. From these studies, it can be concluded that the conversion of syngas with these Ru-based PN^3P catalysts suffers from CO poisoning of the H_2 activation mechanism in these systems, precluding the hydrogenation of CO to take place.

The hydrogenation of CO_2 on the other hand takes place readily, and both complexes **1** and **2** are highly active catalysts for the hydrogenation of CO_2 to formate in the presence of the base DBU. TONs in excess of 30,000 have been achieved with complex **2**, which appears to show better stability compared to complex **1** at lower catalyst loadings. Further catalytic evaluations of these intriguing pincer complexes are underway.

ASSOCIATED CONTENT

Supporting Information

The Supporting Information is available free of charge at https://pubs.acs.org/doi/10.1021/acs.inorgchem.3c04001.

Materials and methods, synthetic procedures, NMR spectra, and SC-XRD (PDF)

Accession Codes

CCDC 2260612 contains the supplementary crystallographic data for this paper. These data can be obtained free of charge via www.ccdc.cam.ac.uk/data_request/cif, or by emailing data_request@ccdc.cam.ac.uk, or by contacting The Cambridge Crystallographic Data Centre, 12 Union Road, Cambridge CB2 1EZ, UK; fax: +44 1223 336033.

AUTHOR INFORMATION

Corresponding Authors

James D. Nobbs − *Institute of Sustainability for Chemicals, Energy and Environment (ICSE2), Agency for Science, Technology and Research (A*STAR), Singapore 627833, Republic of Singapore;* orcid.org/0000-0002-4237-2772; Email: james_nobbs@isce2.a-star.edu.sg

George J.P. Britovsek − *Department of Chemistry, Imperial College London, London W12 0BZ, United Kingdom;* orcid.org/0000-0001-9321-4814; Email: g.britovsek@imperial.ac.uk

Authors

Matthew D. Morton − *Department of Chemistry, Imperial College London, London W12 0BZ, United Kingdom*

Boon Ying Tay − *Institute of Sustainability for Chemicals, Energy and Environment (ICSE2), Agency for Science, Technology and Research (A*STAR), Singapore 627833, Republic of Singapore*

Justin J.Q. Mah − *Institute of Sustainability for Chemicals, Energy and Environment (ICSE2), Agency for Science, Technology and Research (A*STAR), Singapore 627833, Republic of Singapore;* orcid.org/0000-0002-1521-8753

Andrew J.P. White − *Department of Chemistry, Imperial College London, London W12 0BZ, United Kingdom*

Martin van Meurs − *Institute of Sustainability for Chemicals, Energy and Environment (ICSE2), Agency for Science, Technology and Research (A*STAR), Singapore 627833, Republic of Singapore;* orcid.org/0000-0002-8816-3458

Complete contact information is available at: https://pubs.acs.org/10.1021/acs.inorgchem.3c04001

Notes

The authors declare no competing financial interest.

ACKNOWLEDGMENTS

We gratefully acknowledge BP and the Agency for Science, Technology & Research (A*STAR) for funding this work (grant C231218005). We thank Solvay for a generous donation of ClP^{t}Bu$_2$ and Johnson Matthey for the donation of $RuCl_3$.

REFERENCES

(1) Xie, J.; Olsbye, U. The Oxygenate-Mediated Conversion of CO_x to Hydrocarbons - On the Role of Zeolites in Tandem Catalysis. *Chem. Rev.* **2023**, *123*, 11775−11816.

(2) Gao, R.; Zhang, C.; Jun, K.-W.; Kim, S. K.; Park, H.-G.; Zhao, T.; Wang, L.; Wan, H.; Guan, G. Transformation of CO_2 into liquid fuels and synthetic natural gas using green hydrogen: A comparative analysis. *Fuel* **2021**, *291*, No. 120111.

(3) Li, Y.; Zeng, L.; Pang, G.; Wei, X.; Wang, M.; Cheng, K.; Kang, J.; Serra, J. M.; Zhang, Q.; Wang, Y. Direct conversion of carbon dioxide into liquid fuels and chemicals by coupling green hydrogen at high temperature. *Appl. Catal. B: Environ.* **2023**, *324*, No. 122299.

(4) Federsel, C.; Jackstell, R.; Beller, M. State-of-the-art catalysts for hydrogenation of carbon dioxide. *Angew. Chem., Int. Ed.* **2010**, *49*, 6254−6257.

(5) Jessop, P. G.; Joó, F.; Tai, C.-C. Recent advances in the homogeneous hydrogenation of carbon dioxide. *Coord. Chem. Rev.* **2004**, *248*, 2425−2442.

(6) Leitner, W. Carbon Dioxide as a Raw Material: The Synthesis of Formic Acid and Its Derivatives from CO_2. *Angew. Chem., Int. Ed.* **1995**, *34*, 2207−2221.

(7) Moret, S.; Dyson, P. J.; Laurenczy, G. Direct synthesis of formic acid from carbon dioxide by hydrogenation in acidic media. *Nat. Commun.* **2014**, *5*, 4017.

(8) Rohmann, K.; Kothe, J.; Haenel, M. W.; Englert, U.; Holscher, M.; Leitner, W. Hydrogenation of CO_2 to Formic Acid with a Highly Active Ruthenium Acriphos Complex in DMSO and DMSO/Water. *Angew. Chem., Int. Ed.* **2016**, *55*, 8966−8969.

(9) Deka, T. J.; Osman, A. I.; Baruah, D. C.; Rooney, D. W. Methanol fuel production, utilization, and techno-economy: a review. *Environ. Chem. Lett.* **2022**, *20*, 3525−3554.

(10) Ulmer, U.; Dingle, T.; Duchesne, P. N.; Morris, R. H.; Tavasoli, A.; Wood, T.; Ozin, G. A. Fundamentals and applications of photocatalytic CO_2 methanation. *Nat. Commun.* **2019**, *10*, 3169.

(11) Bowker, M. Methanol Synthesis from CO_2 Hydrogenation. *ChemCatChem.* **2019**, *11*, 4238−4246.
(12) Shulenberger, A. M.; Jonsson, F. R.; Ingolfsson, O.; Tran, K.-C., Process For Producing Liquid Fuel From Carbon Dioxide And Water. US 8198338, 2012.
(13) Asinger, F. *Methanol - Chemie- und Energierohstoff*. Springer-Verlag: Berlin, 1986.
(14) Olah, G. A.; Goeppert, A.; Prakash, G. K. S. *Beyond Oil and Gas: The Methanol Economy*. Wiley-VCH: Weinheim, 2006.
(15) Kar, S.; Goeppert, A.; Prakash, G. K. S. Catalytic Homogeneous Hydrogenation of CO to Methanol via Formamide. *J. Am. Chem. Soc.* **2019**, *141*, 12518−12521.
(16) Kaithal, A.; Werle, C.; Leitner, W. Alcohol-Assisted Hydrogenation of Carbon Monoxide to Methanol Using Molecular Manganese Catalysts. *JACS Au* **2021**, *1*, 130−136.
(17) Ryabchuk, P.; Stier, K.; Junge, K.; Checinski, M. P.; Beller, M. Molecularly Defined Manganese Catalyst for Low-Temperature Hydrogenation of Carbon Monoxide to Methanol. *J. Am. Chem. Soc.* **2019**, *141*, 16923−16929.
(18) Sen, R.; Goeppert, A.; Prakash, G. K. S. Homogeneous Hydrogenation of CO_2 and CO to Methanol: The Renaissance of Low-Temperature Catalysis in the Context of the Methanol Economy. *Angew. Chem., Int. Ed.* **2022**, *61*, No. e202207278.
(19) Khusnutdinova, J. R.; Garg, J. A.; Milstein, D. Combining Low-Pressure CO_2 Capture and Hydrogenation To Form Methanol. *ACS Catal.* **2015**, *5*, 2416−2422.
(20) Kar, S.; Sen, R.; Kothandaraman, J.; Goeppert, A.; Chowdhury, R.; Munoz, S. B.; Haiges, R.; Prakash, G. K. S. Mechanistic Insights into Ruthenium-Pincer-Catalyzed Amine-Assisted Homogeneous Hydrogenation of CO_2 to Methanol. *J. Am. Chem. Soc.* **2019**, *141*, 3160−3170.
(21) Rezayee, N. M.; Huff, C. A.; Sanford, M. S. Tandem amine and ruthenium-catalyzed hydrogenation of CO_2 to methanol. *J. Am. Chem. Soc.* **2015**, *137*, 1028−1031.
(22) Kothandaraman, J.; Goeppert, A.; Czaun, M.; Olah, G. A.; Prakash, G. K. Conversion of CO_2 from Air into Methanol Using a Polyamine and a Homogeneous Ruthenium Catalyst. *J. Am. Chem. Soc.* **2016**, *138*, 778−781.
(23) Curley, J. B.; Hert, C.; Bernskoetter, W. H.; Hazari, N.; Mercado, B. Q. Control of Catalyst Isomers Using an N-Phenyl-Substituted $RN(CH_2CH_2P^iPr_2)_2$ Pincer Ligand in CO_2 Hydrogenation and Formic Acid Dehydrogenation. *Inorg. Chem.* **2022**, *61*, 643−656.
(24) Kar, S.; Sen, R.; Goeppert, A.; Prakash, G. K. S. Integrative CO_2 Capture and Hydrogenation to Methanol with Reusable Catalyst and Amine: Toward a Carbon Neutral Methanol Economy. *J. Am. Chem. Soc.* **2018**, *140*, 1580−1583.
(25) Filonenko, G. A.; van Putten, R.; Schulpen, E. N.; Hensen, E. J. M.; Pidko, E. A. Highly Efficient Reversible Hydrogenation of Carbon Dioxide to Formates Using a Ruthenium PNP-Pincer Catalyst. *ChemCatChem.* **2014**, *6*, 1526−1530.
(26) Guan, C.; Pan, Y.; Ang, E. P. L.; Hu, J.; Yao, C.; Huang, M.-H.; Li, H.; Lai, Z.; Huang, K.-W. Conversion of CO_2 from air into formate using amines and phosphorus-nitrogen PN^3P-Ru(II) pincer complexes. *Green Chem.* **2018**, *20*, 4201−4205.
(27) Li, H.; Goncalves, T. P.; Zhao, Q.; Gong, D.; Lai, Z.; Wang, Z.; Zheng, J.; Huang, K. W. Diverse catalytic reactivity of a dearomatized PN^3P*-nickel hydride pincer complex towards CO_2 reduction. *Chem. Commun.* **2018**, *54*, 11395−11398.
(28) Tanaka, R.; Yamashita, M.; Nozaki, K. Catalytic hydrogenation of carbon dioxide using Ir(III)-pincer complexes. *J. Am. Chem. Soc.* **2009**, *131*, 14168−14169.
(29) Tanaka, R.; Yamashita, M.; Chung, L. W.; Morokuma, K.; Nozaki, K. Mechanistic Studies on the Reversible Hydrogenation of Carbon Dioxide Catalyzed by an Ir-PNP Complex. *Organometallics* **2011**, *30*, 6742−6750.
(30) Pan, Y.; Guan, C.; Li, H.; Chakraborty, P.; Zhou, C.; Huang, K. W. CO_2 hydrogenation by phosphorus-nitrogen PN^3P-pincer iridium hydride complexes: elucidation of the deactivation pathway. *Dalton Trans* **2019**, *48*, 12812−12816.
(31) Khusnutdinova, J. R.; Milstein, D. Metal-ligand cooperation. *Angew. Chem., Int. Ed.* **2015**, *54*, 12236−12273.
(32) Alig, L.; Fritz, M.; Schneider, S. First-Row Transition Metal (De)Hydrogenation Catalysis Based On Functional Pincer Ligands. *Chem. Rev.* **2019**, *119*, 2681−2751.
(33) Gunanathan, C.; Milstein, D. Bond activation and catalysis by ruthenium pincer complexes. *Chem. Rev.* **2014**, *114*, 12024−12087.
(34) Mathis, C. L.; Geary, J.; Ardon, Y.; Reese, M. S.; Philliber, M. A.; VanderLinden, R. T.; Saouma, C. T. Thermodynamic Analysis of Metal-Ligand Cooperativity of PNP Ru Complexes: Implications for CO_2 Hydrogenation to Methanol and Catalyst Inhibition. *J. Am. Chem. Soc.* **2019**, *141*, 14317−14328.
(35) Nobbs, J. D.; Sugiarto, S.; See, X. Y.; Cheong, C. B.; Aitipamula, S.; Stubbs, L. P.; van Meurs, M. Tetramethylphosphinane as a new secondary phosphine synthon. *Nat. Commun.* **2023**, *6*, 85.
(36) He, L.-P.; Chen, T.; Xue, D.-X.; Eddaoudi, M.; Huang, K.-W. Efficient transfer hydrogenation reaction Catalyzed by a dearomatized PN^3P ruthenium pincer complex under base-free Conditions. *J. Organomet. Chem.* **2012**, *700*, 202−206.
(37) Benito-Garagorri, D.; Becker, E.; Wiedermann, J.; Lackner, W.; Pollak, M.; Mereiter, K.; Kisala, J.; Kirchner, K. Achiral and Chiral Transition Metal Complexes with Modularly Designed Tridentate PNP Pincer-Type Ligands Based on N-Heterocyclic Diamines. *Organometallics* **2006**, *25*, 1900−1913.
(38) Salem, H.; Shimon, L. J. W.; Diskin-Posner, Y.; Leitus, G.; Ben-David, Y.; Milstein, D. Formation of Stable trans-Dihydride Ruthenium(II) and 16-Electron Ruthenium(0) Complexes Based on Phosphinite PONOP Pincer Ligands. Reactivity toward Water and Electrophiles. *Organometallics* **2009**, *28*, 4791−4806.
(39) Ogata, O.; Nara, H.; Fujiwhara, M.; Matsumura, K.; Kayaki, Y. N-Monomethylation of Aromatic Amines with Methanol via PN(H)-P-Pincer Ru Catalysts. *Org. Lett.* **2018**, *20*, 3866−3870.
(40) Herrmann, W. A. Organometallic Aspects of the Fischer−Tropsch Synthesis. *Angew. Chem., Int. Ed.* **1982**, *21*, 117−130.
(41) Nelson, G. O.; Sumner, C. E. Synthesis and reactivity of pentamethylcyclopentadienylruthenium formyl and α-hydroxy methyl complexes. *Organometallics* **1986**, *5*, 1983−1990.
(42) Nelson, G. O. (Pentamethylcyclopentadienyl)ruthenium compounds. Synthesis and characterization of $(\eta^5\text{-}C_5Me_5)Ru(CO)_2CH_2OH$. *Organometallics* **1983**, *2*, 1474−1475.
(43) Teets, T. S.; Labinger, J. A.; Bercaw, J. E. A Thermodynamic Analysis of Rhenium(I)−Formyl C−H Bond Formation via Base-Assisted Heterolytic H_2 Cleavage in the Secondary Coordination Sphere. *Organometallics* **2013**, *32*, 5530−5545.
(44) Elowe, P. R.; West, N. M.; Labinger, J. A.; Bercaw, J. E. Transformations of Group 7 Carbonyl Complexes: Possible Intermediates in a Homogeneous Syngas Conversion Scheme. *Organometallics* **2009**, *28*, 6218−6227.
(45) Pan, Y.; Pan, C.; Zhang, Y.; Li, H.; Min, S.; Guo, X.; Zheng, B.; Chen, H.; Anders, A.; Lai, Z.; Zheng, J.; Huang, K. Selective Hydrogen Generation from Formic Acid with Well-Defined Complexes of Ruthenium and Phosphorus-Nitrogen PN^3 -Pincer Ligand. *Chem. - Asian J.* **2016**, *11*, 1357−1360.
(46) Ooyama, D.; Tomon, T.; Tsuge, K.; Tanaka, K. Structural and spectroscopic characterization of ruthenium(II) complexes with methyl, formyl, and acetyl groups as model species in multi-step CO_2 reduction. *J. Organomet. Chem.* **2001**, *619*, 299−304.
(47) Toyohara, K.; Nagao, H.; Mizukawa, T.; Tanaka, K. Ruthenium Formyl Complexes as the Branch Point in Two- and Multi-Electron Reductions of CO_2. *Inorg. Chem.* **1995**, *34*, 5399−5400.
(48) Kelly, J. M.; Vos, J. G. *cis*-$[Ru(bpy)_2(CO)H]^+$: A Possible Intermediate in the Photochemical Production of H_2 from Water Catalyzed by $[Ru(bpy)_3]^{2+}$? *Angew. Chem., Int. Ed.* **1982**, *21* (8), 628−629.
(49) Dombek, B. D. Hydrogenation of carbon monoxide to methanol and ethylene glycol by homogeneous ruthenium catalysts. *J. Am. Chem. Soc.* **1980**, *102*, 6855−6857.

https://doi.org/10.1021/acs.inorgchem.3c04001
Inorg. Chem. 2024, 63, 3393−3401

(50) Walker, H. W.; Ford, P. C. Synthesis and characterization of [PPN][HRu(CO)$_4$] and a convenient route to [PPN][HOs(CO)$_4$]. *J. Organomet. Chem.* **1981**, *214*, C43−C44.
(51) Johnson, B. F. G.; Lewis, J.; Raithby, P. R.; Süss, G. The triruthenium cluster anion [Ru$_3$H(CO)$_{11}$]$^-$: preparation, structure, and fluxionality. *J. Chem. Soc., Dalton Trans.* **1979**, *9*, 1356−1361.
(52) Guntermann, N.; Franciò, G.; Leitner, W. Hydrogenation of CO_2 to formic acid in biphasic systems using aqueous solutions of amino acids as the product phase. *Green Chem.* **2022**, *24*, 8069−8075.
(53) Heldebrant, D. J.; Jessop, P. G.; Thomas, C. A.; Eckert, C. A.; Liotta, C. L. The reaction of 1,8-diazabicyclo[5.4.0]undec-7-ene (DBU) with carbon dioxide. *J. Org. Chem.* **2005**, *70*, 5335−5338.

https://doi.org/10.1021/acs.inorgchem.3c04001
Inorg. Chem. 2024, 63, 3393−3401